

Color antisymmetric ghost propagator and the one loop vertex renormalization

Sadataka FURUI

*School of Science and Engineering, Teikyo University
1-1 Toyosatodai, Utsunomiya, 320-8551 Japan*

Color matrix elements of the ghost triangle diagram that appears in the triple gluon vertex and the ghost-ghost-gluon triangle diagram that appears in the ghost-gluon-ghost vertex are calculated. The ghost-ghost-gluon triangle contains a loop consisting of two color diagonal ghost and one gluon and a loop consisting of two color antisymmetric ghost and one gluon. Consequently the pQCD argument in the infrared region based on the one particle irreducible diagram should be modified.

Consequences in the Kugo-Ojima color confinement and the QCD running coupling are discussed.

§1. Introduction

In 1971 't Hooft¹⁾ showed that in mass-less Yang-Mills field theory, non-gauge invariant regulator fields can be incorporated provided in the limit of high regulator mass gauge invariance can be restored by means of finite numbers of counter terms including ghost fields and longitudinally polarized gauge fields. After this work, Taylor²⁾ pointed out that if the charge carried by the ghost and the gauge field are the same, the Ward identity in the QED i.e. $Z_1/Z_2 = 1$ where Z_1 is the vertex renormalization factor and Z_2 is the matter field wave function renormalization factor, can be extended to the QCD as $Z_1/Z_3 = Z_{\bar{\psi}\psi A}/Z_\psi$ where Z_3 is the gluon wave function renormalization factor, Z_ψ is the matter field wave function renormalization factor and $Z_{\bar{\psi}\psi A}$ is the vertex renormalization factor of the matter field.

In these arguments vertices in the tree level are considered and the ghost propagators were assumed to be color diagonal. The ghost propagator is defined as the Fourier transform (FT) of the matrix element of the inverse Faddeev-Popov operator.

$$\begin{aligned} FT[D_G^{ab}(x, y)] &= FT\langle tr(\Lambda^a \{(\mathcal{M})^{-1}\}_{xy} \Lambda^b) \rangle \\ &= \delta^{ab} D_G(q^2), \end{aligned}$$

where $\mathcal{M} = -\partial_\mu D_\mu$, and $\{ \}_{xy}$ means the matrix value. We define the ghost dressing function $G(q^2)$ as $q^2 D_G(q^2)$. In Dyson-Schwinger(DS) approach, $G(q^2)$ at 0 momentum behaves as $\sim (q^2)^{-\kappa}$ and that of gluon dressing function $Z(q^2)$ behaves as $\sim (q^2)^{2\kappa}$.³⁾

In the lattice simulation,^{4),5),6),7)} we calculate the overlap to get the color diagonal ghost propagator

$$D_G(q) = \frac{1}{N_c^2 - 1} \frac{1}{V} tr \left\langle \delta^{ab} (\langle \Lambda^a \cos q \cdot x | f_c^b(x) \rangle + \langle \Lambda^a \sin q \cdot x | f_s^b(x) \rangle) \right\rangle$$

and color antisymmetric ghost propagator

$$\phi^c(q) = \frac{1}{\mathcal{N}} \frac{1}{V} \text{tr} \left\langle f^{abc} (\langle \Lambda^a \cos q \cdot x | f_s^b(x) \rangle - \langle \Lambda^a \sin q \cdot x | f_c^b(x) \rangle) \right\rangle$$

where $\mathcal{N} = 2$ for $SU(2)$ and 6 for $SU(3)$. Here $f_c^b(x)$ and $f_s^b(x)$ are the solution $f^b(x) = \mathcal{M}[U]^{-1} \rho^b(x)$, where U is the lattice link variable, with $\rho_c^b(x) = \frac{1}{\sqrt{V}} \Lambda^b \cos q \cdot x$ and $\rho_s^b(x) = \frac{1}{\sqrt{V}} \Lambda^b \sin q \cdot x$, respectively. We normalize the $SU(3)$ generator Λ^a as $\Lambda^a = \frac{\lambda}{\sqrt{2}}$, where λ is the Gell-Mann's definition. In our notation $\text{tr} \Lambda^a \Lambda^b = \delta^{ab}$.

The lattice study of color antisymmetric ghost propagator in the quenched $SU(2)$ ⁸⁾ and unquenched $SU(3)$ ^{5),6),7)} are motivated by an analysis in the local composite operator(LCO) approach based on the symmetry under the BRST(Becchi, Rouet, Stora and Tyutin) transformation.^{9),11)} Presence of $\langle f^{abc} \bar{c}^b c^c \rangle$ condensates was expected to manifest itself in the color anti-symmetric ghost propagator. The ghost condensates as the on-shell BRST partner of A^2 condensates was also discussed in.¹⁰⁾ In the study of unquenched $SU(3)$,^{5),6),7)} modulus of the color antisymmetric ghost propagator is found to be relatively large and its infrared singularity characterized by $\alpha'_G \sim 0.9$ is larger than that of the color diagonal ghost propagator $\alpha_G \sim 0.25$.⁵⁾ However, an analysis of quenched $SU(3)$ of 56^4 lattice,⁷⁾ showed that the modulus of color antisymmetric ghost propagator is small and its sample variation is large.

These data suggest that the ghost propagator of $SU(2)$ and $SU(3)$ are qualitatively different, although the gluon propagator of the two are similar, and that the presence of the dynamical quark affects the color antisymmetric ghost propagator.

In the momentum subtraction scheme (\widetilde{MOM} scheme), the running coupling in Coulomb gauge and in Landau gauge are calculated by the product of color diagonal ghost dressing function squared and the gluon propagator. The running coupling in Landau gauge is

$$\alpha_s(q) = q^6 D_G(q)^2 D_A(q)$$

where $D_A(q)$ is the gluon propagator in 4-dimensional space and that in Coulomb gauge is,

$$\alpha_I(\mathbf{q}) = \mathbf{q}^5 D_G(\mathbf{q})^2 D_A^{tr}(\mathbf{q})$$

where $D_A^{tr}(\mathbf{q})$ is the 3-dimensional transverse gluon propagator.

In Coulomb gauge, the color-Coulomb potential defines another running coupling $\alpha_{Coul}(\mathbf{q}) = \frac{11N_c - 2N_f}{12N_c} q^2 V_{Coul}(\mathbf{q})$. Since we do not fix A_0 , the variation of $\alpha_{Coul}(\mathbf{q})$ at infrared is large.

We observed that the running coupling in Landau gauge $\alpha_s(q^2)$ has a peak around 2.3 near $q = 0.4\text{GeV}$ but is strongly suppressed below 0.4GeV, but that in Coulomb gauge $\alpha_I(\mathbf{q})$ shows freezing to a constant around 3.¹²⁾ This qualitative difference is expected to be due to the difference of the ghost propagator which is 3 dimensional and instantaneous in the Coulomb gauge but 4 dimensional and propagating in the 4th direction in the Landau gauge.

In usual perturbative QCD(pQCD), ghost is assumed to be color diagonal, which is valid at high energy. In a study of Gribov horizon, Zwanziger introduced a real Bose (ghost) field $\phi_\mu^{ab}(x)$ and the additional action^{13),14)}

$$\begin{aligned}
S &= S_{cl} + \gamma S_1 + S_2 \\
S_{cl} &= \frac{1}{4} \sum_{\mu,\nu,a} \int d^4x (F_{\mu\nu}^a(x))^2 \\
S_1 &= -(2C)^{-1} \int \int d^4x d^4y \text{tr} A_\mu(x) \mathcal{M}[A]^{-1} A_\nu(y) \\
S_2 &= \int d^4x \left(\frac{1}{2} \phi_\mu^{ab} \mathcal{M}^{bd}[A] \phi_\mu^{ad} + i\gamma^{1/2} C^{-1/2} f^{abd} \phi_\mu^{ad} A_\mu^b \right), \tag{1.1}
\end{aligned}$$

for restricting the gauge configuration in the fundamental modular region. Here C is the value of $SU(3)$ Casimir operator of fundamental representation.

In the Gribov-Zwanziger Lagrangian, the equation of motion of ϕ_μ^{ad} becomes¹⁵⁾

$$(D_\mu \phi_\nu)^{ab} = \partial_\mu \phi_\nu^{ab} f^{acd} A_\mu^c \phi_\nu^{db} \tag{1.2}$$

and its solution is

$$\phi_\mu^{ab} = -\frac{\gamma^2}{\sqrt{2}} f^{abc} \mathcal{M}[A]^{-1} A_\mu^c \tag{1.3}$$

When A_μ^c is replaced as $q_\mu c^c$, where c^c is the ghost field and f^{deh} is multiplied,

$$f^{deh} \phi_\mu^{ab} = -\frac{\gamma^2}{\sqrt{2}} (\delta^{ae} \delta^{bh} - \delta^{be} \delta^{ah}) \mathcal{M}[A]^{-1} q_\mu c^c \tag{1.4}$$

The color antisymmetric ghost $\phi^c(q)$ multiplied by the momentum q_μ and f^{deh} is similar to the Zwanziger's ghost ϕ_μ^{ab} . In an analytical one-loop calculation, based on the Gribov-Zwanziger Lagrangian, including two additional ghost field denoted by $\{\phi_\mu^{ab}, \bar{\phi}_\mu^{ab}\}$ and $\{\omega_\mu^{ab}, \bar{\omega}_\mu^{ab}\}$, infrared freezing of the running coupling $\alpha_s(q)$ was demonstrated.¹⁵⁾ Although the Zwanziger's ghost ϕ_μ^{ab} was introduced for restricting the gauge configuration into the fundamental modular region, its relation to the A^2 condensates was discussed in ref.¹⁶⁾ Although the color antisymmetric ghost multiplied by the momentum q_μ and f^{deh} and the ϕ_μ^{ab} are different, we expect similar corrections to the infrared exponents of the gluon propagator and the ghost propagator through the color antisymmetric ghost propagator in the Landau gauge, when it is incorporated properly.

Organization of the paper is as follows. In sect.2 we study the triple gluon vertex and the ghost-gluon-ghost vertex in one loop. In sect.3 the contribution of the ghost loop in the gluon propagator is investigated and in sect.4 the contribution of the gluon-ghost-ghost loop in the ghost propagator is studied. Discussion on the quark-gluon vertex, the Kugo-Ojima confinement parameter and QCD running coupling are given in sect.5 and 6. Conclusion and outlook are given in sect.7.

§2. The triple gluon vertex and the ghost-gluon-ghost vertex

In this section we show the contribution of the color antisymmetric ghost propagator in the triple gluon vertex and the ghost-gluon-ghost vertex.

The triple gluon vertex defined as Fig.1 in the pQCD is given by the tree level diagram (Fig.2), ghost loop diagram (Fig.3) and the gluon loop diagram (Fig.4)

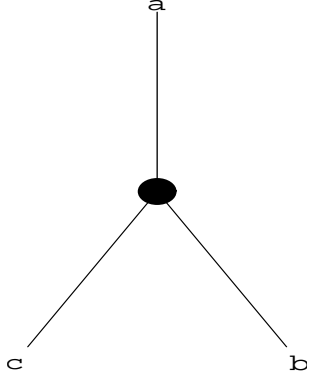


Fig. 1. The triple gluon vertex.

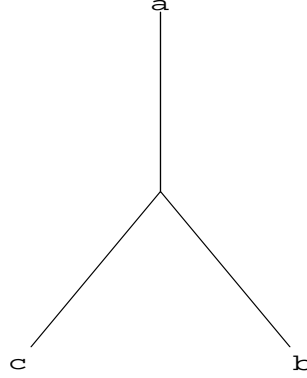


Fig. 2. The bare triple gluon vertex.

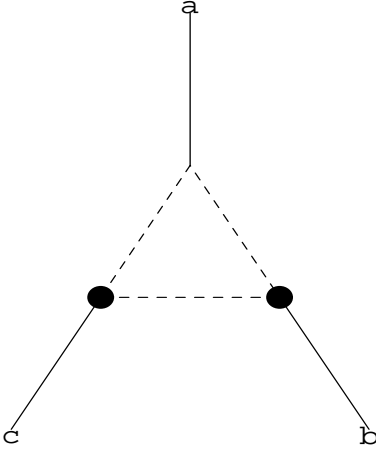


Fig. 3. The dressed triple gluon vertex. The dashed line is a ghost and the thin line is a gluon.

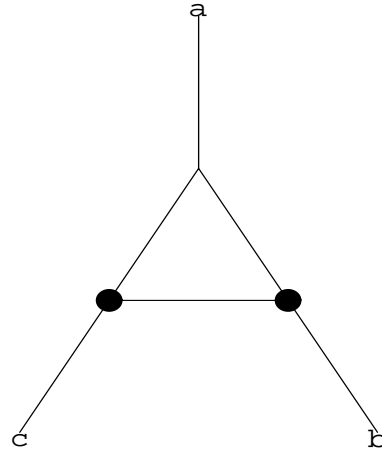


Fig. 4. The triple gluon vertex. The thin lines are gluon.

The color indices of the ghost loop in the triple gluon vertex are assigned as in Fig.5. We express the ghost propagator which is assigned as d as a combination of the color diagonal and color antisymmetric pieces:

$$\delta^{a''c''} D_G(k) + 2f^{a''c''d} \phi_d(k). \quad (2.1)$$

The same combination is assumed for the ghost assigned as h . At the three edges of the triangle the color factor

$$f^{a''a'a} f^{b''b'b} f^{c''c'c} \quad (2.2)$$

is multiplied.

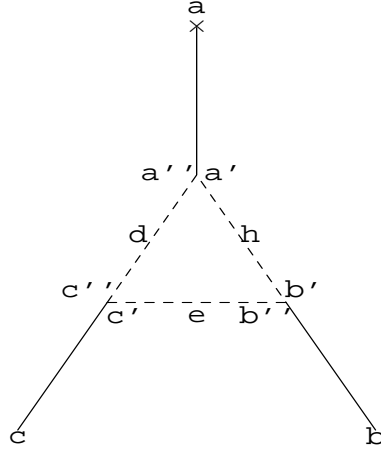


Fig. 5. The triple gluon vertex. The dashed line is a ghost and the thin line is a gluon.

The ghost-gluon-ghost vertex is expressed as Fig.6 and its tree level diagram is Fig.7. In one-loop level, the ghost-ghost-gluon loop as shown in Fig.8 contributes. The assignment of the color indices is shown in Fig.9.

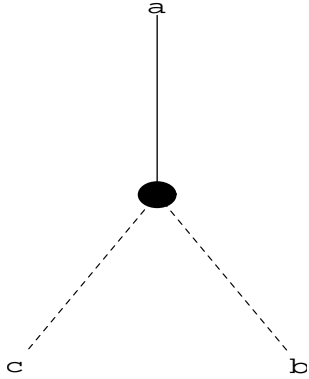


Fig. 6. The gluon-ghost-ghost vertex. The dashed line is a ghost and the thin line is a gluon.

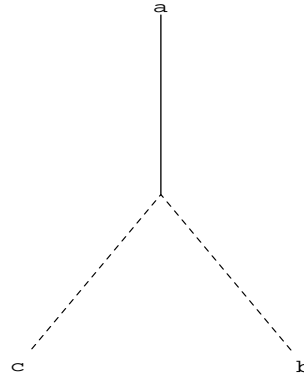


Fig. 7. The gluon-ghost-ghost vertex. The dashed line is a ghost and the thin line is a gluon.

In the calculation of the color matrix element of one loop vertex diagram of Fig.5 and 9, we fix a, b, c and make a summation on color indices $a', a'', b', b'', c', c'', d, e, h$. The matrix elements of the quark gluon vertices are proportional to f^{abc} which are

- $f^{123} = 1$
- $f^{147} = f^{246} = f^{345} = f^{516} = f^{257} = f^{637} = \frac{1}{2}$
- $f^{458} = f^{678} = \frac{\sqrt{3}}{2}$

Using the definition $D_{c'b''} = D_e$, $D_{a'b'} = D_h$ and $D_{a''c''} = D_d$, we obtain in the case of $SU(2)$ the coefficients as in Table I. In this table abc and deh are the $SU(2)$

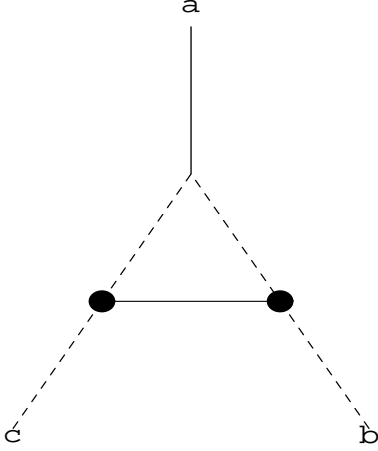


Fig. 8. The gluon-ghost-ghost vertex. The dashed line is a ghost and the thin line is a gluon.

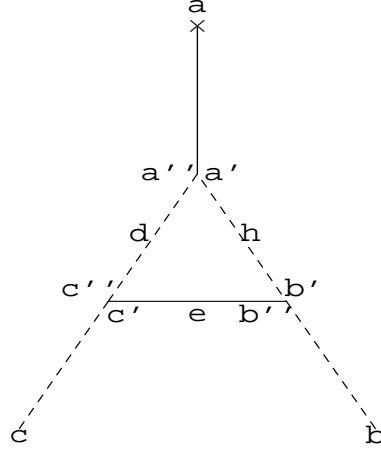


Fig. 9. The gluon-ghost-ghost vertex. The dashed line is a ghost and the thin line is a gluon.

color indices, $D_h D_d D_e$ are all color diagonal $D_h \phi_d \phi_e$, and $D_e \phi_h \phi_d$ are one propagator assigned as D_h or D_e are color diagonal but the rest are color antisymmetric.

When deh are not elements of the Cartan subalgebra, there appear terms proportional to $\phi\phi\phi$ but the coefficient is purely imaginary and both plus sign terms and minus sign terms appear and they cancel.

abc	deh	$D_h D_d D_e$	$D_h \phi_d \phi_e$	$D_d \phi_e \phi_h$	$D_e \phi_h \phi_d$
123	333	-1	-4	0	0

Table I. The $SU(2)$ color matrix elements of the ghost triangle diagram.

In the case of $SU(3)$ we obtain the coefficients which are to be multiplied on f^{abc} as in Table II. The gluon which has the color index in the Cartan subalgebra coupled with a pair of color antisymmetric ghost propagator and the contribution is additive to that of gluon couples with a pair of color diagonal ghost propagator.

Qualitative difference of the color matrix elements of $SU(2)$ and $SU(3)$ comes from the anomaly cancelling equation of the triangle diagram

$$\text{tr}\{\{A^a, A^b\}A^c\} = 0 \quad (2.3)$$

where $\{\}$ is the anti-commutator is satisfied for $SU(2)$ but not for $SU(3)$.

The coefficients of $D\phi\phi$ terms of f^{458} and f^{678} differ only in their signs. When color indices $deh=333$ and $abc=123$, the same structure as in the $SU(2)$ appears. But when $deh=888$ and $abc=147$ since f^{458} and f^{678} are only the coefficient that do not vanish when coupled to the color source 8, the color antisymmetric pair appears in the link d and e .

In the case of unquenched $SU(3)$ configuration with Kogut-Susskind fermion MILC $_f$, the ratio of the dressing function $q^2\phi(q)/G(q)$ at $q \sim 0.18\text{GeV}$ is about 0.2 and at $q \sim 0.4\text{GeV}$ is 0.08.^{6),7)} While in the case of quenched $SU(2)$, the ratio at $q \sim 0.25\text{GeV}$ is about 0.1^{8),17)} and at $q \sim 0.4\text{GeV}$ is 0.05-0.06.^{5),8),17)}

abc	deh	$D_h D_d D_e$	$D_h \phi_d \phi_e$	$D_d \phi_e \phi_h$	$D_e \phi_h \phi_d$
123	888	-1.5	-1.5	1.5	1.5
	333	-1.5	-4.5	0	0
	833	-1.5	0	-0.5	0
	383	-1.5	0	0	-0.5
	338	-1.5	-4.5	0	0
	838	-1.5	0	0	1.5
	883	-1.5	-1.5	0	0
	388	-1.5	0	1.5	0
147	888	-1.5	0	0	1.5
	333	-1.5	-1	1	-0.5
	338	-1.5	-1	0	$-\sqrt{3}/2$
	383	-1.5	$-\sqrt{3}$	$-\sqrt{3}$	-0.5
	833	-1.5	0	1	$\sqrt{3}/2$
	883	-1.5	0	$-\sqrt{3}$	$\sqrt{3}/2$
	838	-1.5	0	0	1.5
	388	-1.5	$-\sqrt{3}$	0	$\sqrt{3}/2$
458	888	-1.5	4.5	0	0
	333	-1.5	-1.5	1	1
	338	-1.5	-1.5	0	0
	383	-1.5	$-\sqrt{3}/2$	$-\sqrt{3}$	1
	833	-1.5	$-\sqrt{3}/2$	1	$-\sqrt{3}$
	388	-1.5	$-\sqrt{3}/2$	0	0
	883	-1.5	-4.5	$-\sqrt{3}$	$-\sqrt{3}$
	838	-1.5	$-\sqrt{3}/2$	0	0
453	888	-1.5	-1.5	0	0
	333	-1.5	-4.5	1	1
	833	-1.5	$\frac{3\sqrt{3}}{2}$	1	$\sqrt{3}$
	383	-1.5	$-\frac{3\sqrt{3}}{2}$	$\sqrt{3}$	1
	338	-1.5	-4.5	$-2\sqrt{3}$	$-2\sqrt{3}$
	838	-1.5	$\frac{3\sqrt{3}}{2}$	$-2\sqrt{3}$	0
	883	-1.5	-1.5	$\sqrt{3}$	$\sqrt{3}$
	388	-1.5	0	$-\frac{3\sqrt{3}}{2}$	$-2\sqrt{3}$
678	888	-1.5	-4.5	0	0
	333	-1.5	-1.5	1	1
	338	-1.5	-1.5	0	0
	383	-1.5	$\sqrt{3}/2$	$\sqrt{3}$	1
	833	-1.5	$\sqrt{3}/2$	1	$\sqrt{3}$
	388	-1.5	$\sqrt{3}/2$	0	0
	883	-1.5	-4.5	$\sqrt{3}$	$\sqrt{3}$
	838	-1.5	$\sqrt{3}/2$	0	0

Table II. The $SU(3)$ color matrix elements of the ghost triangle.

§3. The ghost loop in the gluon propagator

In one loop order the vacuum polarization tensor that contributes to the gluon self energy consists of a) quark loop, b) ghost loop (Fig.10), c) gluon tadpole and d) gluon loop (Fig.11). In b) there is a ghost-gluon-ghost vertex and in d) there is a triple gluon vertex in the two loop order in which the color antisymmetric ghost

could contribute. In this section we study the effect of the ghost loop on the gluon propagator.

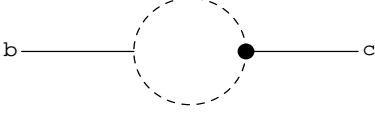


Fig. 10. The gluon propagator dressed by ghost propagator.

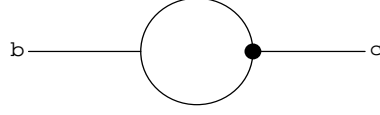


Fig. 11. The gluon propagator dressed by gluon propagator.

Product of the color antisymmetric ghost propagator contributes in the ghost-loop diagram as shown in Fig.12. The cross means a coupling to the quark loop as shown in Fig.13 or to gluon loops. The quark loop or the gluon loop can couple to other gluons, and among the ghost propagator specified by d, e and h , one is color diagonal and the other two are color antisymmetric. The color matrix elements we calculated in the triple gluon vertex imply that if the ghost propagator which does not couple with the gluon of color index a is color diagonal and the rest are color antisymmetric, the color index a should belong to the Cartan subalgebra, so that the matrix element becomes real.

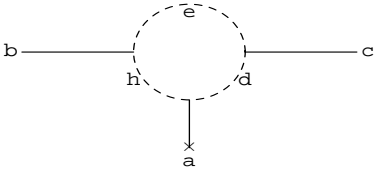


Fig. 12. The ghost loop contribution in the gluon propagator. The dashed line is a ghost. The x indicates the dressing of a gluon whose color index is a .

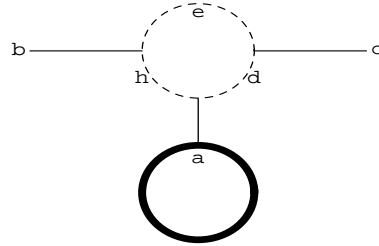


Fig. 13. The ghost loop contribution in the gluon propagator. The dashed line is a ghost and the thick line is a quark.

But since other gluons can couple to the quark loop, the color index a is not necessarily in the Cartan subalgebra. The propagator is proportional to f^{abc} and since the signs of the color matrix element of TableII are random, its contribution is expected to be small and the color mixing of gluons would be small. Lattice simulations also indicate that the gluon propagator is diagonal in color.

§4. The ghost-ghost-gluon loop in the ghost propagator

In one loop order, the ghost self energy is given by the gluon-ghost loop shown in Fig.14.

In two loop order, the ghost-ghost-gluon loop contributes in which a pair of color antisymmetric ghost propagator and the gluon propagator are incorporated.. We consider a production of the color antisymmetric ghost pair production from a gluon of color index a . The propagator shown in Fig.15 is proportional to f^{abc} and when making a trace it vanishes. However, a product of these propagators shown in

Fig.16 does not vanish and contribute in the dressing of the external ghosts of the ghost-gluon-ghost vertex.

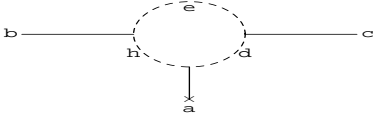


Fig. 14. The ghost propagator.

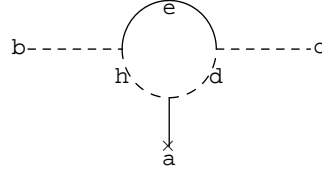


Fig. 15. The dressing of the ghost propagator by the gluon. The dashed line is a ghost the thin line is a gluon. The x indicates dressing of a gluon in Cartan subalgebra.

When the gluon with the color index a can be treated as a background field, that couples to a quark loop, as shown in Fig.17 color antisymmetric ghost propagator contributes. Different from gluon propagator, the color mixing of the ghost is not unfavored from the lattice simulation.

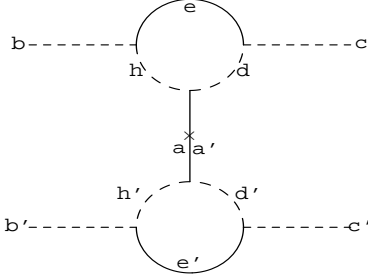


Fig. 16. The two ghost propagator. The x indicates a gluon of color indices $a = a'$ in the Cartan subalgebra.

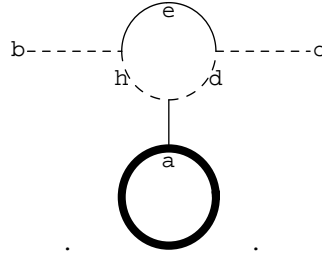


Fig. 17. The dressing of the ghost propagator by the gluon. The dashed line is a ghost the thin line is a gluon and the thick line is a quark.

Dressing of the ghost propagator by the gluon is given by the Fig.14. The integral is expressed as

$$d(b, c) = \int \frac{d^4 q}{(2\pi)^4} \delta^{bc} \left(\frac{\delta_{\mu\nu} q_\mu q_\nu}{(p-q)^2 q^{2(1+\kappa)}} - \frac{q_\mu q_\nu (p-q)_\mu (p-q)_\nu}{(p-q)^4 q^{2(1+\kappa)}} \right) Z_3((p-q)^2). \quad (4.1)$$

When the $Z_3((p-q)^2)$ is taken as a constant, the formulae in²²⁾ gives

$$d(b, c) \propto K_2(1 + \kappa, 1, p)p^2 - (K_2(1 + \kappa, 2, p)p^4 - 2L_2(1 + \kappa, 2, p)p^4 + M_3(1 + \kappa, 2, p)p^4) \quad (4.2)$$

where

$$\begin{aligned}
\int d^4q \frac{q_\mu q_\nu}{q^{2a}(P-q)^{2b}} &= K_1(a, b, p)p_\mu p_\nu + K_2(a, b, p)p^2 \delta_{\mu\nu}, \\
\int d^4q \frac{q_\mu q_\nu q_\rho}{q^{2a}(p-q)^{2b}} &= L_1(a, b, p)p_\mu p_\nu p_\rho + L_2(a, b, p)p^2(p_\mu \delta_{\nu\rho} + p_\nu \delta_{\rho\mu} + p_\rho \delta_{\mu\nu}), \\
\int d^4q \frac{q_\mu q_\nu q_\rho q_\sigma}{q^{2a}(p-q)^{2b}} &= M_1(a, b, p)p_\mu p_\nu p_\rho p_\sigma \\
&+ M_2(a, b, p)p^2(\delta_{\mu\nu} p_\rho p_\sigma + \delta_{\mu\rho} p_\nu p_\sigma + \delta_{\mu\sigma} p_\rho p_\mu + \delta_{\nu\rho} p_\mu p_\sigma + \delta_{\nu\sigma} p_\rho p_\mu + \delta_{\rho\sigma} p_\mu p_\nu) \\
&+ M_3(a, b, p)p^4(\delta_{\mu\nu} \delta_{\rho\sigma} + \delta_{\mu\rho} \delta_{\nu\sigma} + \delta_{\mu\sigma} \delta_{\rho\nu})
\end{aligned} \tag{4.3}$$

According to the ansatz of DS equation, exponent of the ghost dressing function $\kappa \sim \alpha_G$ and it is related to the exponent of the gluon dressing function α_D as $-2\kappa \sim \alpha_D$.⁴⁾ When $\kappa = 0.5$ corresponding to the infrared finite gluon propagator, the integral becomes

$$\delta^{bc} d(b, c) = -\frac{6.26379}{(p^2)^{0.5}} - \left(\frac{6.57974}{(p^2)^{0.5}} - 2 \frac{3.94784p^2}{(p^2)^{0.5}} - \frac{1.12795p^4}{(p^2)^{0.5}} \right) \tag{4.4}$$

Recent analysis of the exponent of the gluon dressing function of lattices with long time axis is given in ref.¹⁸⁾ In reality κ in the infrared and the ultraviolet could be different and the above numerical values should be regarded as a simple estimation.

The loop integral of the ghost-ghost-gluon triangle is expressed as

$$\begin{aligned}
I(p, a, b, c) &= \int \frac{d^4q}{(2\pi)^4} \left(\delta_{\mu\nu} - \frac{(p-q)_\mu (p-q)_\nu}{(p-q)^2} \right) \frac{Z_3((p-q)^2)}{(p-q)^2} \\
&\times \left(\frac{\delta^{a''c''}}{q^{2(1+\kappa)}} + 2i f^{a''c''d} \phi_d(q) \right) (-g f^{a''aa'} q_\mu) \\
&\times \left(\frac{\delta^{b'a'}}{q^{2(1+\kappa)}} + 2i f^{b'a'h} \phi_h(q) \right) (-g f^{b''bb'} q_\nu) \\
&\times \sum_x (\text{loop term})(t^a)_{xx}.
\end{aligned} \tag{4.5}$$

where the quark loop contribution is expressed as the loop term.

The color matrix elements are given in Table IV, where D_{Ae} indicates the color diagonal gluon propagator. The coherent contribution $D_e \phi \phi$ from $dh=88$ and 33 suggests the color mixing occurs in the infrared region. The contribution of the color antisymmetric ghost propagator would be enhanced in the unquenched lattice simulation, when the quark loop becomes a source of the color antisymmetric pair.

The exponent of the color diagonal ghost dressing function α_G is ~ 0.25 ,^{5),4)} and that of color antisymmetric ghost dressing function defined at $q \sim 0.4\text{GeV}$ is $\alpha'_G \sim 0.9$.⁶⁾ By using formulae in ref²²⁾ and assuming $Z_3((p-q)^2)$ constant in the relevant integration region which is we obtain

$$\begin{aligned}
I(p, a, b, c) &\propto f^{abc} (c_1 K_2(2(1+\kappa), 1, p)p^2 + c_2 K_2(2(1+\kappa'), 1, p)p^2) \\
&- (c_1 (K_2(2(1+\kappa), 2, p)p^4 - 2L_2(2(1+\kappa), 2, p)p^4 + M_3(2(1+\kappa), 2, p)p^4) \\
&- (c_2 (K_2(2(1+\kappa'), 2, p)p^4 - 2L_2(2(1+\kappa'), 2, p)p^4 + M_3(2(1+\kappa'), 2, p)p^4) \tag{4.6}
\end{aligned}$$

abc	dh	$D_h D_d D_{Ae}$	$D_{Ae} \phi_h \phi_d$
321	88	1.5	-1.5
	33	1.5	-4.5
	83	1.5	0
	38	1.5	0
854	88	1.5	-4.5
	33	1.5	-1.5
	83	1.5	$\sqrt{3}/2$
	38	1.5	$\sqrt{3}/2$
876	88	1.5	-4.5
	33	1.5	-1.5
	83	1.5	$-\sqrt{3}/2$
	38	1.5	$-\sqrt{3}/2$

Table III. The $SU(3)$ color matrix elements of the ghost-ghost-gluon triangle.

where c_1 is the color matrix element of $D_{Ae} D_h D_d$ and c_2 is the color matrix element of $D_{Ae} \phi_h \phi_d$. Using $\kappa = 0.5$ for D_h, D_d and $\kappa' = 0.9$ for ϕ_h, ϕ_d , we obtain

$$\begin{aligned}
I(p, a, b, c) &\propto f^{abc} \left(c_1 \left(-\frac{\infty}{p^2} \right) + c_2 \left(-\frac{6.1196}{p^{2.8}} \right) \right. \\
&\quad \left. - \left(c_1 \left(-\frac{\infty}{p^2} - 2\frac{\pi^2}{4p^2} + \frac{\pi^2}{16p^2} \right) \right) \right. \\
&\quad \left. - \left(c_2 \left(-\frac{2.203}{p^{3.8}} - 2\frac{8.81215}{p^{3.8}} + \frac{2.03985}{p^{3.8}} \right) \right) \right). \tag{4.7}
\end{aligned}$$

We remark that the diverging terms cancel with each other.

The dressed ghost propagator can be incorporated in the ghost loop in the gluon propagator as shown in Fig.18, and modify the infrared behavior of the gluon propagator in the lattice Landau gauge.

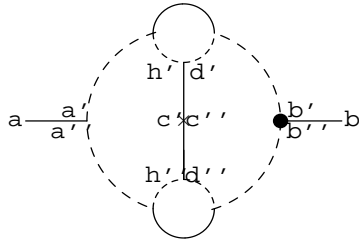


Fig. 18. The gluon propagator with ghost loop. The dashed line is a ghost the thin line is a gluon. The x indicates dressing of the gluon in Cartan subalgebra.

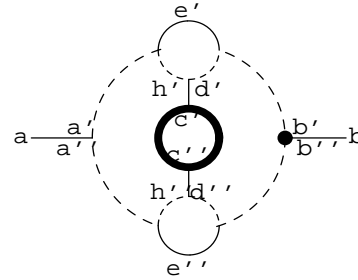


Fig. 19. The gluon propagator with ghost loop and quark loop contributions. The dashed line is a ghost the thin line is a gluon and the loop of thick line is a quark.

The loop of quarks in the fundamental representation yields $tr(t^{c'} t^{c''}) = \delta^{c', c''} \frac{1}{2}$.

The sum of color indices becomes

$$2g(a, b, c', c'') = \sum_{a', a'', b', b''} \delta^{c', c''} f^{aa'a''} f^{bb'b''} f^{c'a'b'} f^{c''a''b''} \quad (4.8)$$

gives $4.5\delta^{ab}$. The $D_{Ae}\phi_h\phi_d$ loop contribution denoted by c_2 exists only when $c', c'' = 3, 8$, but there is no restriction to the $D_{Ae}D_hD_d$ loop contribution denoted by c_1 , but the infrared singularity of the c_2 term is stronger than the c_1 term..

c—ab	11	22	33	44	55	66	77	88
3	-0.25	-0.25	2.25	0.5	0.5	0.5	0.5	0.75
8	0.75	0.75	0.75	0	0	0	0	2.25

Table IV. Color matrix elements of the gluon propagator.

§5. The quark-gluon vertex

The quark-gluon vertex is calculated from the longitudinal photon quark coupling

$$q_\mu \Gamma_\mu(p, q) = G(q^2)[(1 - H(q, p + q))S^{-1}(p) - S^{-1}(1 - H(q, p + q))] \quad (5.1)$$

where $G(q^2)$ is the ghost dressing function and $H(q, p + q)$ is the ghost-quark scattering kernel. In the continuum theory, the ghost-quark scattering kernel in the quark-gluon vertex was discussed in ref.¹⁹⁾ Its role in the DS approach was examined in ref.²⁰⁾ and in the lattice simulation in ref.²¹⁾

In the quark-gluon vertex, a ghost-triangle couples with an external gluon and two internal gluons couple to the quark as shown in Fig.20.

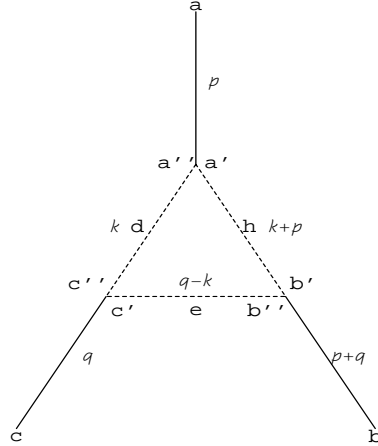


Fig. 20. The ghost triangle. The color indices of the external gluons and internal ghosts and the momentum assignments.

The color of the external gluon is specified by a and two internal gluons are specified by b, c . When the ghost-quark scattering kernel is approximated by a

dressed gluon exchange, the amplitude of the quark-gluon vertex becomes

$$\begin{aligned}
M(p, s, a, x, y) &= \int \frac{d^4 k}{(2\pi)^4} \int \frac{d^4 q}{(2\pi)^4} \\
&\times \left(\frac{\delta^{a''c''}}{k^{2(1+\kappa)}} + 2if^{a''c''d}\phi_d(k) \right) (-gf^{a''aa'k}) \\
&\times \left(\frac{\delta^{c'b''}}{(q-k)^{2(1+\kappa)}} + 2if^{c'b''e}\phi_e(q-k) \right) (-gf^{c''cc'}(q-k)) \\
&\times \left(\frac{\delta^{b'a'}}{(k+p)^{2(1+\kappa)}} + 2if^{b'a'h}\phi_h(k+p) \right) (-gf^{b''bb'}(k+p)) \\
&\times (igt^c)_{xz}(igt^b)_{zy}Z_2((s-q)^2) \frac{-i(\not{s}-\not{q})+M}{(s-q)^2+M^2} \\
&\times (\delta_{\mu\nu} - \frac{q_\mu q_\nu}{q^2}) \frac{Z_3(q^2)}{q^2} \\
&\times (\delta_{\eta\delta} - \frac{(q+p)_\eta(q+p)_\delta}{(q+p)^2}) \frac{Z_3((q+p)^2)}{(q+p)^2}. \tag{5.2}
\end{aligned}$$

It would be important to remark that the color antisymmetric ghost does not appear as an external line, but it appears in the vertex as an internal line. The gluon dressing expressed by a cross can be contracted as $\delta^{c'c''}$ and becomes a propagator in the Cartan subalgebra. This could effectively introduce the ghost condensates effect.(Choice of a specific color direction.)

§6. Effects on the Kugo-Ojima color confinement parameter and the running coupling

Kugo and Ojima²³⁾ constructed a two-point function $u^{ab}(q)$ from the Lagrangian in the Landau gauge that satisfies BRST symmetry. They claimed that if its value at momentum zero is -1, it is an evidence of the color confinement.

$$\begin{aligned}
&(\delta_{\mu\nu} - \frac{q_\mu q_\nu}{q^2})u^{ab}(q^2) \\
&= \frac{1}{V} \sum_{x,y} e^{-ip(x-y)} \langle \text{tr} \left(A^{a\dagger} D_\mu \mathcal{M}^{-1} [A_\nu, A^b] \right)_{xy} \rangle, \tag{6.1}
\end{aligned}$$

$$u^{ab}(0) = -\delta^{ab}c$$

In this argument and in the proof of the Slavnov-Taylor identity on the ratio of the vertex renormalization factor and the wave function renormalization factor²⁴⁾

$$\frac{Z_1}{Z_3} = \frac{\tilde{Z}_1}{\tilde{Z}_3} = \frac{Z_{\bar{\psi}\psi A}}{Z_\psi}$$

the ghost propagator is assumed to be color diagonal.

Replacement of

$$\langle c^a(x)\bar{c}^b(y) \rangle = D_G(x-y)\delta^{ab} + f^{abc}\phi^c(x-y) \quad (6.2)$$

does not affect the argument in the tree level since the expectation value of $\phi(x-y)$ is 0. However, when there is a ghost color mixing of the type Fig.15

$$\langle c(A_\nu \times \bar{c}) \rangle_{1PI} \neq iq_\rho \langle (A_\rho \times c)(A_\nu \times \bar{c}) \rangle_{1PI}. \quad (6.3)$$

Thus, when one writes

$$\langle D_\mu c \bar{c} \rangle = \langle \partial_\mu c \bar{c} \rangle + \langle (A_\mu \times c) \bar{c} \rangle \equiv iq_\mu (1 + F(q^2)) \frac{1}{q^2 G(q^2)} \quad (6.4)$$

where

$$\begin{aligned} \langle c \bar{c} \rangle &\equiv -\frac{1}{q^2 G(q^2)}, \\ \langle (A_\mu \times c) \bar{c} \rangle_{1PI} &\equiv -iq_\mu F(q^2) \\ \langle D_\mu c (A_\mu \times \bar{c}) \rangle &= \langle \partial_\mu c \bar{c} \rangle \langle c (A_\mu \times \bar{c}) \rangle_{1PI} + \langle (A_\mu \times c) (A_\nu \times \bar{c}) \rangle_{1PI} \\ &\neq (\delta_{\rho\mu} - \frac{q_\mu q_\rho}{q^2}) \langle c (A_\mu \times \bar{c}) \rangle_{1PI} \end{aligned} \quad (6.5)$$

and $u(0) \neq F(0) = G(0) - 1$, or there should be a contribution of the ghost propagator of the type Fig.15 between c and \bar{c} which is not proportional to δ^{ab} .

In the S-matrix theory, the ghost intermediate state cancels the intermediate states with non-physically polarized gluon. The longitudinal gluon with polarization vector $-ip_\mu$ couples with a set of diagrams of a given order in g and a given number of transverse gluon on mass shell, which are expressed as a circle in the t'Hooft definition, and it was shown that all the contributions cancel out to 0, when ghost are color diagonal.

Our analysis suggests that if the longitudinal gluon makes a pair of color antisymmetric ghost and the loop intersects with the circle, the contribution remains since the contribution of the cut-off denoted by Λ in the t'Hooft definition cancels the color-diagonal ghost contribution. It will give an artificial suppression of the ghost propagator and the QCD running coupling.

No infrared suppression occurs in $\alpha_I(\mathbf{q})$ since the longitudinal gluon polarized in the 4th direction does not contribute in the three dimensional calculation.

The color indices of the color antisymmetric ghost pair could be ordered if there is a long range background gluon field that couples to the pair. In this case eq.(6.5) would be satisfied and the Kugo-Ojima parameter c becomes close to 1.

There is no direct proof that the quark loop introduces the ordering, but the difference of the Binder cumulant of the color antisymmetric ghost propagator of the quenched simulation and the unquenched simulations^{5),6),7)} strongly suggests this effect. The temperature dependence of the parameter c ⁷⁾ could also be explained by this mechanism.

§7. Discussion and outlook

We discussed that the deviation of the Kugo-Ojima parameter c from 1 and the infrared suppression of the effective coupling $\alpha_s(q)$ in Landau gauge could be due to the color antisymmetric ghost propagator.

In the case of Coulomb gauge, the ghost dressing function is three dimensional and no dissipation of the flow occurs and the running coupling freezes.

The lattice Landau gauge results show some discrepancies from the results of DS equation in the infrared exponents of the ghost propagator and the gluon propagator. We investigated the possibility that this discrepancy comes from the color-mixing of the ghost propagator induced by the ghost-gluon-ghost triangle diagram. A study in the DSE is left as a future study.

The color antisymmetric ghost pair couples to a gluon whose color is in the Cartan subalgebra. The lattice data suggest that the gluon in the Cartan subalgebra couples with a dynamical quark loop, which make a difference of the color antisymmetric ghost propagator of quenched configurations and that of unquenched configurations.

We studied also the contribution of ghost triangle diagram in the quark-gluon vertex. For the estimation of the latter effect, it is necessary to perform the two-loop calculation and it is left to the future.

Acknowledgements

Main part of this work was done at the Department of Theoretical Physics of University of Graz in August 2007. The author thanks Kai Schwenzer and Reinhard Alkofer for helpful and enlightening discussions in Graz and Hideo Nakajima for the collaboration in the lattice simulation cited in this paper. Thanks are also due to the Austrian Academic Exchange Service for the support of the author's stay in Graz and the Japan Society for the Promotion of Science (JSPS) for the support through the Scientist Exchange Program that enabled the collaboration.

References

- 1) G. 't Hooft, Nucl. Phys. **B33**, 173 (1971).
- 2) J.C. Taylor, Nucl. Phys. **B33**, 436 (1971).
- 3) R. Alkofer and L. von Smekal, Phys. Rept. **353**281 (2001); hep-ph/0007355.
- 4) S. Furui and H. Nakajima, Phys. Rev. D**69**,074505 (2004).
- 5) S. Furui and H. Nakajima, Phys. Rev. D**73**, 094506(2006); hep-lat/0612009.
- 6) S. Furui and H. Nakajima, Braz. J. Phys.**37**,186 (2007); hep-lat/0609024.
- 7) S. Furui and H. Nakajima, Phys. Rev. D**76**,054509 (2007); hep-lat/0612009.
- 8) A. Cucchieri, T. Mendes and A. Mihara, Phys. Rev. D**72**,094505 (2005); hep-lat/0408034.
- 9) D. Dudal et al., J. High Energy Phys. **0306** 003, (2003)
- 10) K.I. Kondo, Phys. Lett. **B514** 335(2001), hep-th/0105299.
- 11) V.E.R. Lemes, M.S. Sarandy and S.P. Sorella, Annals Phys. 308 (2003) 1; hep-th/0210077
- 12) S. Furui and H. Nakajima, PoS (Lattice2007)301,(2007); arXiv:0708.1421
- 13) D. Zwanziger, Nucl. Phys. **B323**,513 (1989).
- 14) D. Zwanziger, Nucl. Phys. **B412**,657 (1994).
- 15) J.A. Gracey, J. High Energy Phys. **05** 052, (2006); hep-ph/0605077.
- 16) D. Dudal, R.F. Sobreiro, S.P. Sorella and H. Verschelde, Phys. Rev. D**72**,014016

- (2005),hep-th/0502183.
- 17) J.C.R. Bloch, A. Cucchieri, K. Langfeld and T. Mendes, Nucl. Phys. **B**(Proc. Supp.)**119**,736(2003); hep-lat/0209040.
 - 18) O. Oliveira and P. Silva, Braz. J. Phys.**37**,201 (2007).
 - 19) H. Pagels, Phys. Rev. D**15**, 2991 (1977).
 - 20) C.S. Fischer and R. Alkofer, Phys. Rev. D**67**,094020 (2003).
 - 21) J. Skullerud and A. Kizilersü, J. High Energy Phys. **09**, 013 (2002); hep-ph/0205318.
 - 22) A. Alkofer, C.S. Fischer, H. Reinhardt and L. von Smekal, Phys. Rev. D**68**,045003 (2003); hep-th/0304134.
 - 23) T. Kugo and I. Ojima, Prog. Theor. Phys. Suppl. **66**, 1 (1979).
 - 24) T. Kugo, hep-th/9511033.